Sensors and Materials, Vol. 10, No. 5 (1998) 263–273
MYU Tokyo

S & M 0330

Improved Ion-Conducting Layer Replacing the Insulator in a Capacitive Chemical Semiconductor Sensor

Tigran Gabusjan, Lars Bartholomäus and Werner Moritz

Humboldt-University Berlin, Walther-Nernst-Institut of Physical and Theoretical Chemistry, Bunsenstr. 1, 10117 Berlin, Germany

(Received December 24, 1996; accepted March 19, 1998)

Key words: chemical sensor, semiconductor, ionic conductor, capacitance, field effect, LaF_3, MIS, thin layer, CV measurement, impedance

The influence of heterovalent doping of LaF_3 with SrF_2 on the electrical behavior of a silicon-based chemical sensor and ion conductivity of the doped LaF_3 layer were investigated. An improved quality of field effect devices was achieved using a $La_{(0.964)}Sr_{(0.036)}F_{(2.96)}$ layer instead of the insulator. Capacitance voltage curves of metal/ionic conductor/semiconductor (MICS) devices are much steeper than for conventional metal/insulator/semiconductor (MIS) devices. It was proven that interface, not insulator-bulk, capacitances dominate the behavior of the field effect device. The results obtained can be applied to field effect devices other than chemical sensors.

1. Introduction

A chemically sensitive semiconductor sensor was introduced as an ion-sensitive field-effect transistor (ISFET) in 1970 by Bergveld.[1] In numerous studies, the more simple electrolyte/insulator/semiconductor (EIS) structure has been used, which is identical in construction to the gate region of the ISFET.[2] These sensors are characterized by capacitance/voltage (CV) measurements. For potentiometric sensors, high-precision measurement is necessary, since an error of only 1 mV in the potential shift determined corresponds to an error in concentration of 4% (exchange of one electron). Therefore the steepness of the CV curves is of great importance for achieving accurate measurements. The shape of the CV curves is determined by the carrier concentration in the silicon

substrate, the thickness of the insulator and the density of interface states.[3] Improved CV behavior of EIS sensors has been achieved using porous silicon.[4] The substitution of the insulator by the ionic conductor LaF_3 which is in direct contact with the silicon without intermediate insulating layers, also leads to a field effect device.[5,6] The resulting fluoride ion sensor was proven to be very stable and advantageous for precise measurements, considering its very steep CV curve. It was shown that the density of surface states was very low for the Si/LaF_3 interface. Recently, we developed gas sensors for the determination of oxygen and fluorine or hydrogen fluoride using a Si/LaF_3/Pt structure[7–9] of the MICS type.

Fluoride materials with the tysonite structure (LaF_3) are considered to be some of the best superionic conductors with fluorine ion conductivity. The introduction of heterovalent impurities such as SrF_2 into the LaF_3 leads to a further improvement in the ion conductivity by about two orders of magnitude.[10]

The purpose of this work is to achieve further improvement of the sensor electrical characteristics by influencing ion conductivity in such a way that the interfaces, not the bulk properties of the material, determine the capacitance of the device. We employed the simultaneous evaporation of LaF_3 and SrF_2 to produce a thin layer exhibiting high ion conductivity onto the silicon. Following gate metallization the electrical properties of the gas sensor were determined. Impedance spectroscopy and DC measurements were used to analyze the electrical properties of the thin layer structure.

2. Materials and Methods

MICS sensor structures were produced using p-type Si with $\rho = 10\ \Omega \cdot$ cm and (111) orientation. Thin films of LaF_3 doped with SrF_2 were prepared by thermal evaporation in a vacuum from LaF_3:SrF_2 pellets. The content of SrF_2 was 2 wt.%. The vacuum during evaporation was better than 5×10^{-6} mbar, the substrate temperature was 823 K, the rate of evaporation 0.3 – 0.6 nm/s and the film thickness 400 nm. The DC cathode-sputtering method was used to fabricate Pt thin films (30 nm). The ohmic contacts to Si were made with thin films of Al. Samples for electrical conductivity measurements were fabricated on sapphire substrates with Pt contacts to $La_xSr_yF_z$.

For characterization of the sensor structures, high-frequency CV measurements were used. Impedance measurements were carried out in the frequency range of $5 \times 10^{-2} - 10^6$ Hz (IM5d; Zahner Electric, Germany). Electrophysical experiments were conducted in the temperature range of 300 – 573 K. To prevent changes in the surface chemistry at high temperature, the conductivity and CV measurements were carried out under vacuum (10^{-1} Pa). The crystalline structure of $La_xSr_yF_z$ films was investigated by X-ray diffraction measurements. The chemical composition of the film was determined using XPS measurements.

The influence of heating in an oxygen atmosphere (synthetic air) on the electrical behavior of the structures was investigated in the temperature range from 300 to 623 K.

3. Results

3.1 *Sensor properties following preparation under vacuum*

The improvement in accumulation capacitance and steepness of high-frequency CV curves for $Si/LaF_3/Pt$ sensors with a direct-contact Si/LaF_3 (MICS) compared to a $Si/SiO_2/Si_3N_4/LaF_3/Pt$ structure is shown in Fig. 1 (curves a) and b)). As discussed in ref. (11) the increased steepness is due to three different reasons. First, a very low density of surface states ($< 10^{10}$ cm^{-2} eV^{-1}) was observed at the Si/LaF_3 interface. This is related to a surprisingly high reproducibility of the flat-band voltage for independent preparations (only ± 60 mV). Second, the higher dielectric constant of the LaF_3 leads to an increased capacitance in accumulation for comparable layer thicknesses. Third, the high ionic conductivity of the LaF_3 leads to a voltage drop across the bulk of the LaF_3 layer equal to zero for DC voltage. The insulating properties of the field effect device are determined here by the blocking ion conductor/semiconductor interface. The total voltage drop V_G for the field effect device is split into band bending v_S in the semiconductor and voltage drop across the insulator (Q_S/C_{IS}). In eqs. (1) and (2) [3] u_S and u_B are the normalized surface and bulk potential, respectively, Q_S is the normalized space charge and C_{IS} is the insulator capacitance under DC conditions:

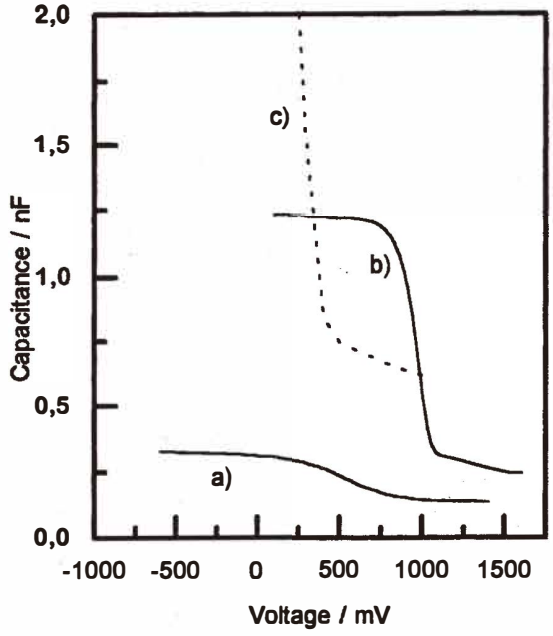

Fig. 1. Capacitance/voltage curves of field effect structures ($A_{Pt} = 3.1$ mm^2); $f = 10$ kHz. a) $Si/SiO_2/Si_3N_4/LaF_3$ /Pt (SiO_2 $d = 76$ nm; Si_3N_4 $d = 80$ nm). b) Si/LaF_3 /Pt. c) $Si/La_xSr_yF_z/Pt$.

$$v_S = u_S - u_B \tag{1}$$

$$V_G = -\frac{Q_S}{C_{IS}} + \frac{kT}{q}\left(u_S - u_B\right). \tag{2}$$

For the MICS structure, C_{IS} is equivalent to the interface capacitance and for a MIS structure, to the capacitance of the insulator layer. Because of the much higher value of the interface capacitance compared to that of thin insulator layers, the relation between the surface potential in the silicon and the external gate voltage (eq. (2)) is different between MICS devices and classical structures with insulator layers (MIS), leading to steeper curves.[11]

The aim of doping the LaF_3 layer with SrF_2 was to improve the AC behavior (capacitance) in addition to the DC behavior, based on the increased ion conductivity known for heterovalent doped material.[10] The increase in the capacitance for $Si/La_xSr_yF_z/Pt$ samples having the same area is shown in Fig. 1, curve c). Since the capacitance is so high that it cannot be seen in the accumulation region of the CV curve, Fig. 1 is rescaled in Fig. 2. The expected improvement in capacitance is clearly shown, but there is a drawback in the fact that, in contrast to the theoretical prediction, the capacitance in accumulation does not become constant. We found that the reason for this behavior is a leakage of DC current.

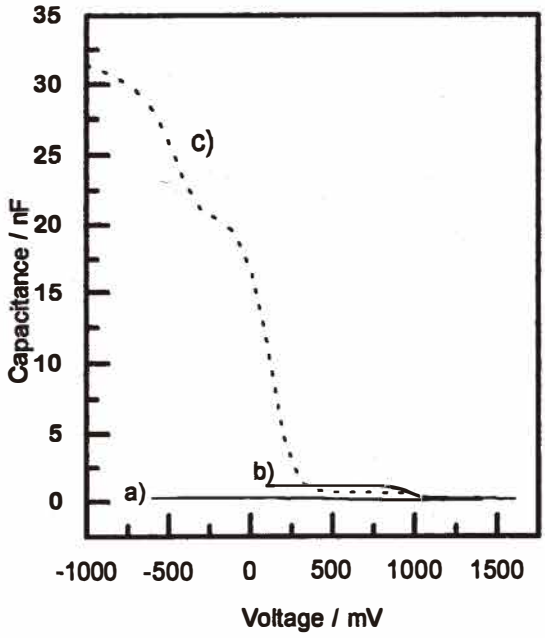

Fig. 2. Capacitance/voltage curves of field effect structures (rescaled). a) $Si/SiO_2/Si_3N_4/LaF_3/Pt$. b) $Si/LaF_3/Pt$. c) $Si/La_xSr_yF_z/Pt$.

3.2 *DC behavior of the sensor*

The DC current behavior of a Si/$La_xSr_yF_z$/Pt sample is shown in Fig. 3, curve a). For very high current it is easy to understand that the CV characteristics are disturbed. Therefore, we tried to improve the sensor behavior with different treatments which do not change the sensitivity of our sensor. The most efficient approach was thermal treatment in synthetic air. In Fig. 3, the strong reduction in current through the sensor after heating it in synthetic air at 623 K for 4 h is shown.

This behavior can be explained by the chemisorption of oxygen and OH^- groups from air. The chemisorption of oxygen and OH^- groups by these films after heating in air was proved by X-ray and XPS measurements. It leads to the formation of additional negative charge in the film and reduces the conductivity of F^- ions. Furthermore, the Si/LaF_3 contact becomes blocking, which leads to a significant reduction in DC current. After heating the sample in a vacuum at a temperature above 500 K, we again observed an increase in DC current through the structure. Therefore, the process of chemisorption of active gases is reversible.

In Fig. 4 the results of impedance spectroscopy measurements on the Si/$La_xSr_yF_z$/Pt structure are shown. The DC current of nontreated samples acts as a parallel resistance, as is obvious in the low-frequency range. Of course, this description is too simple and therefore, an influence of the heating procedure was also found for higher frequencies. For the nontreated structure, there is no frequency exhibiting a pure capacitive behavior, as would be expected for field effect devices. In contrast, after thermal treatment, there is a large frequency domain (f > 10 Hz) that can be used. It should be noted that the reduced

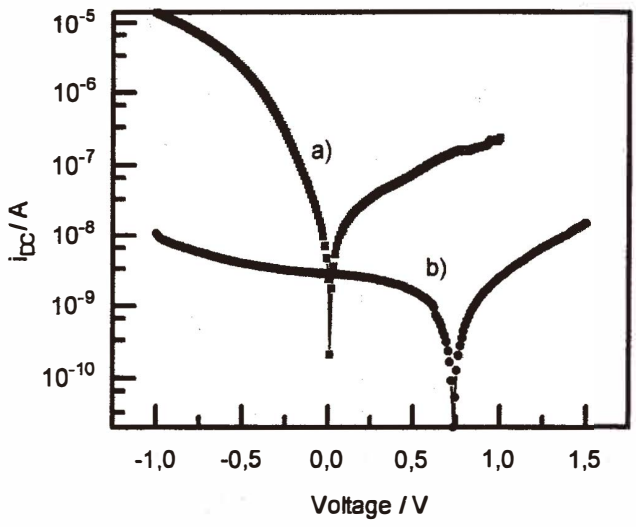

Fig. 3. Influence of heating in air on the DC current of the structure Si/$La_xSr_yF_z$/Pt: a) without thermal treatment; b) after heating the sample in synthetic air for 4 h at 623 K.

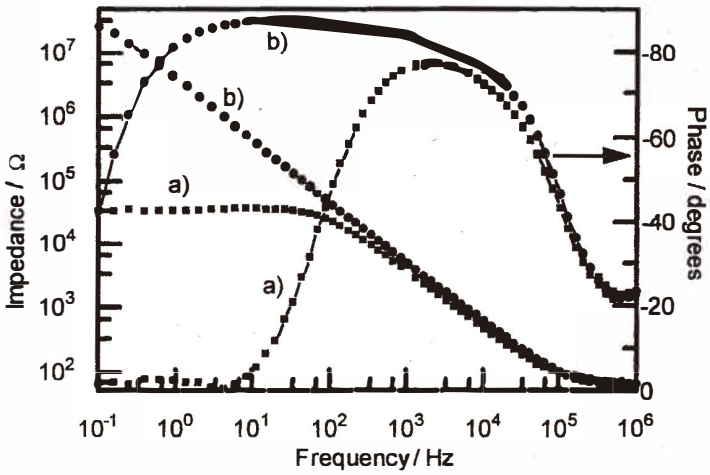

Fig. 4. Impedance spectroscopy for a Si/$La_xSr_yF_z$/Pt probe: a) without thermal treatment; b) after heating the sample in synthetic air for 4 h at 623 K.

phase shift at high frequencies is not common for MIS structures. The reason for this behavior is the very high capacitance of our MICS structures and therefore, the small resistances of the Si bulk and the $La_xSr_yF_z$ bulk are dominant at high frequencies.

3.3 *Properties of the ion-conducting layer*

The composition of the $La_xSr_yF_z$ layer was analyzed using XPS measurements. Apart from some oxygen found in all the samples, the composition of the fluoride ion conductor was proven to be $La_{(0.964)}Sr_{(0.036)}F_{(2.96)}$.

The investigation of the ion conductivity of this doped LaF_3 layer when fabricated onto silicon is not very exact as there are problems with leakage current for DC measurements and additional resistances (silicon bulk and ohmic contact) for high-frequency investigations. Therefore we used $La_{(0.964)}Sr_{(0.036)}F_{(2.96)}$ prepared on an insulating sapphire substrate, and two platinum contacts on top.

The DC measurement of electrical conductance is complicated by the large (1 μC/cm^2) polarization effect in such films, leading to an apparent static dielectric constant of 10^6.[12]

When a step voltage V was applied across the thin film sample the current increased rapidly to a maximum value I(o) and then decayed with time to a steady-state value I(oo) (Fig. 5).

It has been pointed out by Sutter and Norwick[13] that if the polarization results from a space-charge buildup due to blocking electrodes, then the conductance is given by I(o)/V; if it is the result of a dielectric relaxation phenomenon, the true conductance is given by I(oo)/V.

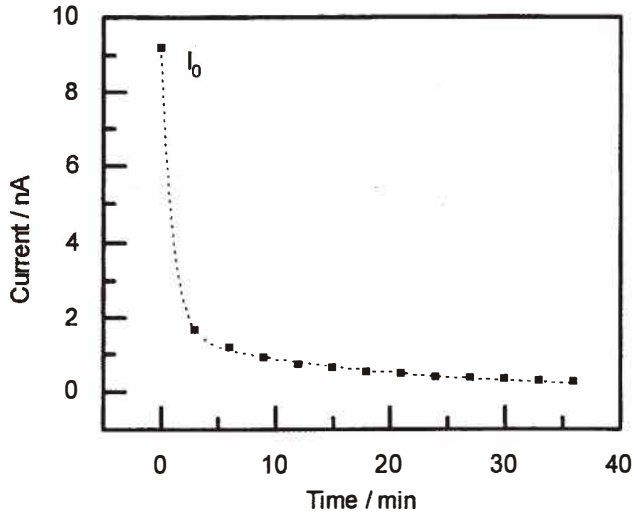

Fig. 5. Time dependence of DC current for a Si/$La_xSr_yF_z$/Pt structure, $U = 2$ V.

In agreement with the results for single-crystal LaF_3 it has been determined that the polarization in these thin films is a space charge effect. A procedure for measuring conductivity is to measure $I(o)$ using a step voltage. Furthermore, we used impedance spectroscopy to investigate the ion conductivity of these samples. Ohmic impedance corresponding to the bulk properties of $La_xSr_yF_z$ was found in the low frequency range of 10 mHz–1 Hz. The results of the two measurements are in good agreement.

The temperature dependence of conductivity σ for thin $La_xSr_yF_z$ films is shown in Fig. 6. The electric conductivity of tysonite, LaF_3, is due to the migration of fluorine anions, according to the vacancy mechanism. Fluorine vacancies are ion current carriers in tysonite structures. We observed a change in the dependence of σ on temperature at $T(c) =$ 420–450 K. In the temperature range 300–600 K, the $\sigma(T)$ curves consist of two regions, and satisfy the Arrhenius-Frenkel equation (eq. (3)), which is in good agreement with the results for single crystals:[10]

$$\sigma T = \sigma_0 \exp\left(-\Delta H(\sigma)/kT\right), \tag{3}$$

where ΔH is the activation enthalpy of conductivity. For the low-temperature region, ΔH = 0.335 eV and for the high-temperature region, $\Delta H = 0.127$ eV.

The conductivity of $La_{(0.964)}Sr_{(0.036)}F_{(2.96)}$ films was determined to be $1.35 - 1.6 \times 10^{-3}$ S/m at 300 K and $1.3 - 2.2 \times 10^{-1}$ S/m at 523 K.

A comparison of the conductivity of $La_xSr_yF_z$ films and LaF_3 films at 300 K shows that the conductivity of doped films is at least two orders of magnitude higher than that of LaF_3

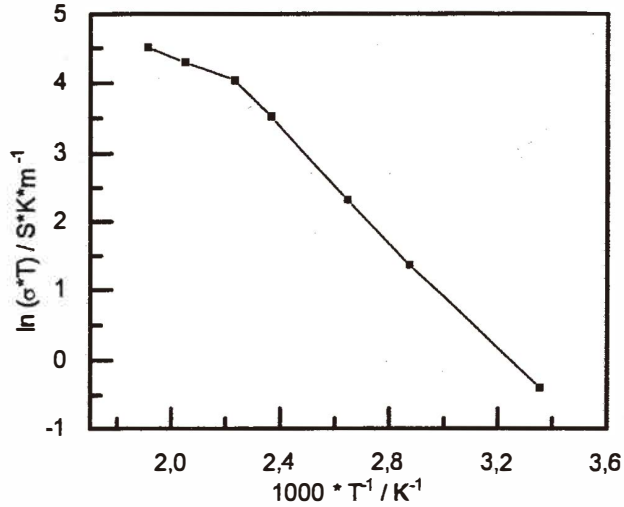

Fig. 6. Temperature dependence of conductivity for $La_{(0.964)}Sr_{(0.036)}F_{(2.96)}$ films (from impedance spectroscopy measurements).

films. (Our measurements were not optimized for this low-conductivity LaF_3, but in the literature, values for polycrystalline layers are 10^{-5}–10^{-7} S/m.[14,15])

3.4 *Sensor characteristics*

For a sensor structure, Si/$La_xSr_yF_z$/Pt, following thermal treatment in synthetic air, an improved CV curve was obtaind, as shown in Fig. 7 (compare with Fig. 2c). As predicted by the MIS theory, in the more negative voltage range, a nearly constant capacitance is dominated by the "insulator" capacitance (here interface capacitance; see below) of the MIS or MICS structure while the space-charge capacitance of the semiconductor is so high that it becomes negligible. This is a very advantageous curve in terms of the determination of gas concentration because the very high steepness of the CV curve reduces the error in potential caused by fluctuations of capacitance.

To prove that sensor properties are not changed by the thermal treatment, the sensitivity to fluorine was investigated. A typical result is shown in Fig. 8. The sensitivity corresponds to the Nernst equation with a formal exchange of half an electron, and is in good agreement with the results for samples not exposed to thermal treatment and not doped with SrF_2.[9] The dynamic behavior is also comparable between the two preparations. The mechanism of the sensor reaction was discussed in ref. (9).

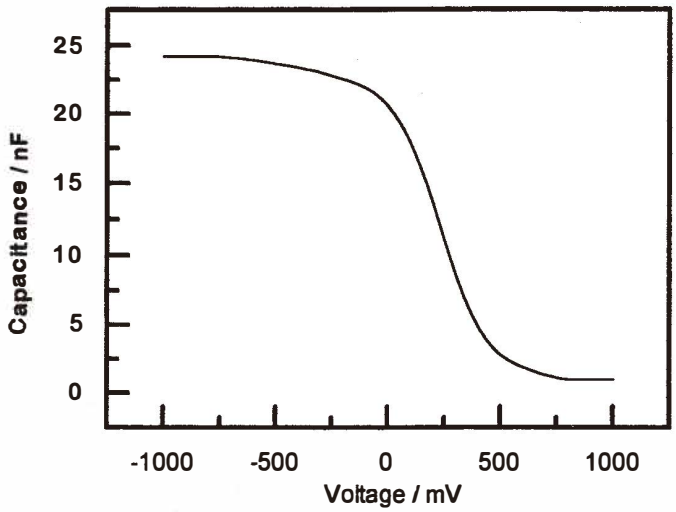

Fig. 7. Capacitance/voltage curve of the field effect structure $Si/La_xSr_yF_z/Pt$ after thermal treatment (A_{Pt} = 3.1 mm^2); f =10 kHz.

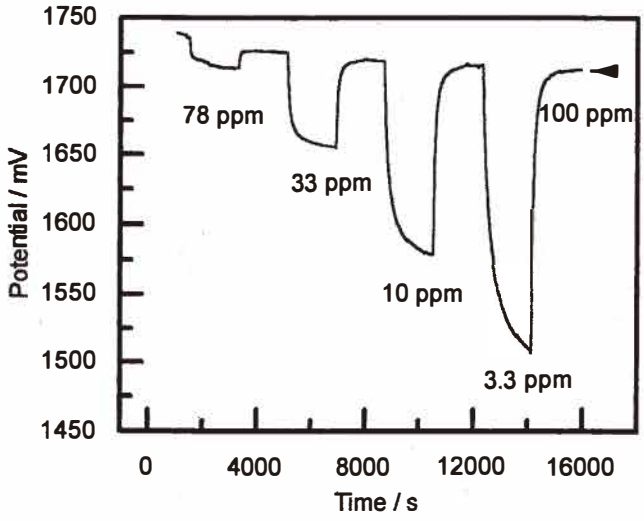

Fig. 8. Response of the field effect structure $Si/La_xSr_yF_z/Pt$ to different concentrations of fluorine.

4. Discussion

Following thermal treatment, the DC current of the sensor structure is small enough to be negligible with respect to the sensor behavior. For the discussion of the electrical behavior of this high-capacitance MICS structure, we use a simplified equivalent circuit, as shown in Fig. 9. Typically for a MIS structure the total capacitance C_{MIS} is determined by the insulator bulk capacitance C_{IS} (4) and the voltage-dependent capacitance of the space-charge region of the semiconductor C_{SC} (5) (surface state charge is neglected here).

$$C_{MIS} = \frac{1}{\frac{1}{C_{SC}} + \frac{1}{C_{IS}}} \tag{4}$$

For the ion-conducting layer, capacitance (2) and resistance (3) can be used for the description of the electrical properties. If there is direct contact between the ionic conductor and the silicon, as in our MICS samples, capacitance (4) can be omitted. The interfaces Si/LaF_3 and Pt/LaF_3 should each be represented by a resistance and a capacitance in parallel, but because of the very high resistance, a simplification leads to one capacitance (1).

For the LaF_3 without heterovalent doping, the ohmic impedance of the layer is high compared to the capacitive impedance for the frequency range of interest and has only a minor influence on the total impedance. At the same time, the interface capacitances of Pt/LaF_3 and Si/LaF_3 are higher than the bulk capacitance of the LaF_3 layer. The total impedance is complex[11] but the value is close to that of the bulk capacitance.

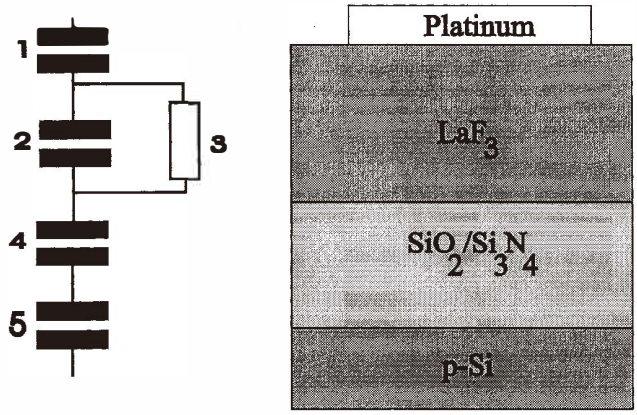

Fig. 9. Schematic of the sensor and equivalent circuit (see text).

For the Si/$La_xSr_yF_z$/Pt structure the high ion conductivity leads to a bulk resistance of typically 80 Ω (gate area 2 mm^2). Compared to a capacitance of 1.3 nF, the bulk impedance is dominated by the resistivity for frequencies up to 1 MHz. Furthermore, the resistance is small compared to the interface capacitances up to about 30 kHz (see Fig. 4). For the structure used it is not possible to distinguish between the Pt/LaF_3 and Si/LaF_3 interfaces. The total capacitance of both was found to be 900 nF/cm^2. This is a value that can be explained by a thin space-charge region formed by a distribution of fluoride ions near the interface.

5. Conclusion

We have shown that the heterovalent doping of LaF_3 by SrF_2 leads to thin layers of $La_xSr_yF_z$ which can be used in a MICS sensor structure with improved electrical properties. At the same time, the behavior of the chemical sensor is not changed. The capacitance of the field effect device is determined by interface capacitances, while the bulk capacitance of the MICS is negligible, leading to much higher capacitances.

The application of this improved behavior should not be restricted to chemical sensors but can also be applied to supercapacitors and other field effect devices.[16]

References

1 P. Bergveld: IEEE Trans. Biomed. Eng. BME-**17** (1970) 342.
2 P. Fabry and L. Laurant-Yvonneau: J. Electroanal. Chem. **286** (1990) 23.
3 E. H. Nicollian and J. R. Brews: MOS Physics and Technology (J. Wiley & Sons, New York, 1982).
4 M. J. Schöning, M. Crott. F. Ronkel, M. Thust, J. W. Schultze, P. Kordos and H. Lüth: Third ICIM/ECSSM'96 (SPIE Volume 2779) p. 275.
5 J. Szeponik and W. Moritz: Sensors and Actuators **2** (1990) 243.
6 W. Moritz, J. Szeponik, F. Lisdat, A. Friebe, S. Krause, R. Hintsche and F. Scheller: Eurosensors V, Rome 30.9.-2.10.1991 and Sensors and Actuators B **7** (1992) 497.
7 S. Krause, W. Moritz and I. Grohmann: Sensors and Actuators B **9** (1992) 191.
8 W. Moritz, S. Krause and I. Grohmann: Eurosensors VII, Budapest 1994 and Sensors and Actuators B **18** (1994) 148.
9 W. Moritz, S. Krause, A. A. Vasiliev, D.Yu. Godovski and V. V. Malyshev: The Fifth International Meeting on Chemical Sensors, Rome 11–14. July 1994 and Sensors and Actuators B **24–25** (1995) 194.
10 N. I. Sorokin and B. P. Sobolev: Crystallography Reports **39** (1994) 810.
11 J. Szeponik, W. Moritz and F. Sellam: Ber. Bunsenges. Phys. Chem. **95** (1991) 1448.
12 C. O. Tiller, A. C. Lilly and B. C. LaRoy: Physical Review B **8** (1973) 4787.
13 P. H. Sutter and A. S. Norwick: J. Appl. Phys. **34** (1963) 734.
14 A. Sher, R. Solomon, K. Lee and M. W. Muller: Phys. Rev. **144** (1966) 593.
15 J. R. Igel, M. C. Wintersgill, J. J. Fontanella, A. V. Chadwick, C. G. Andeen and V. E. Been: J. Phys. C, Solid State Phys. **15** (1982) 7215.
16 A. Sher, W. E. Miller, Y. H. Tsuo, J. A. Moriarty, R. K. Crouch and B. A. Seiber: Appl. Phys. Lett. **34** (1979) 799.